



## Band edge photoluminescence of undoped and doped TlInS<sub>2</sub> layered crystals



O.V. Korolik<sup>a</sup>, S.A.D. Kaabi<sup>a</sup>, K. Gulbinas<sup>b</sup>, N.V. Mazanik<sup>c</sup>, N.A. Drozdov<sup>a</sup>, V. Grivickas<sup>b,\*</sup>

<sup>a</sup> Belarusian State University, Nezalezhnastsi Av. 4, 220030, Minsk, Belarus

<sup>b</sup> Institute of Applied Research, Vilnius University, Sauletekio av. 10, LT-10223, Vilnius, Lithuania

<sup>c</sup> Belarusian State Technology University, Sverdlov st. 13A, 220006, Minsk, Belarus

### ARTICLE INFO

#### Article history:

Received 25 October 2016

Received in revised form

4 January 2017

Accepted 27 March 2017

Available online 31 March 2017

#### Keywords:

TlInS<sub>2</sub>

Layered semiconductor structure

Phase transformations

Doping

Photoluminescence

Low dimension intrinsic excitons

### ABSTRACT

Intrinsic photoluminescence (PL) of undoped and of B-, Ag- or Er-doped TlInS<sub>2</sub> layered single crystals was investigated by confocal spectroscopy. It is found that position and intensity of PL spectral peak at 2.4 eV is vastly dependent on the excitation light incidence and polarization relative to crystallographic directions. For the normal incidence to the layer plane  $k||c$ , a significant Stokes shift between the PL peak in respect to exciton absorption energy is highlighted. The shift increases to 80 meV around the crystal phase transformations region of 200 K. We show that presence of B and Ag impurity do not diminish the intrinsic PL emission while Er atoms incorporation enhances it substantially and modifies a fine excitonic line structure in the ferroelectric phase at low T. The obtained results imply out-of-layer plain oriented 2D excitons in TlInS<sub>2</sub> existing at various crystal phases which are influenced by related interlayer stresses.

© 2017 Elsevier B.V. All rights reserved.

### 1. Introduction

Thallium based dichalcogenides TlInS<sub>2</sub>, TlInSe<sub>2</sub>, TlInTe<sub>2</sub>, TlGaS<sub>2</sub>, TlGaSe<sub>2</sub>, TlGaTe<sub>2</sub> exhibit quasi low dimensionality of layered chain structures. Some crystals possess a number of unique optical, photoelectrical and ferroelectric properties due to specificity in their structure having no parallels with bulk 3D semiconductors or quantum wells. The lattice of TlInS<sub>2</sub> consist of two alternating layer structure twisted by right angle on (001) plain respect to the preceding layer. The layers are linked by bridging Tl atoms located in the trigonal prismatic voids between the In<sub>4</sub>S<sub>10</sub> polyhedron along the [110] and  $\bar{1}\bar{1}0$  of the two  $a,b$  crystallographic lines. Among other dichalcogenide compounds, TlInS<sub>2</sub> and its mixed alloys attracted strong attention for promising potential applications [1–3].

It is a matter of common knowledge that photoluminescence (PL) reflects peculiarities of electronic collective excitations in semiconductors. Nevertheless, in Tl-based layered structures the complexity arises that band-edge in a large extend is constructed by weakly interlayer atomic orbitals resulting in a number of electronic branches within the Brillouin zone. While details of the band structure in TlInS<sub>2</sub> are not established properly, the lowest direct exciton absorption peak has the low absorption coefficient in excess of  $(1-5) \times$

$10^3 \text{ cm}^{-1}$  [3–5]. In addition crystals exhibit lower energy indirect valleys on the conduction band. The interlayer forces are modified by dislocations or by planar stacking fault (PSF) defects. The PSFs occur due to monoclinic layer plain gliding on  $a,b$  lines by 0.5 lattice unit. Another gliding by 0.5 unit in the same direction returns the same lattice structure. Flexibility of layers also manifests by observed crystal phases. The paraelectric normal N-phase was detected in TlInS<sub>2</sub> crystals at RT while the incommensurate I-phase providing quadrupling of the unit cell volume was observed in the range 200–216 K. Below 200 K the TlInS<sub>2</sub> crystal losses inversion symmetry and transforms into the commensurate ferroelectric F-phase. The authors in Ref. [6] also implied that a new weaker F-phase occurs at even lower temperature < 50 K. All observed phases however preserve nearly the pseudo-tetragonal metrics normal to the layer plain  $c$ -axis [1,2].

In other isostructural compound TlGaSe<sub>2</sub> the experiments have revealed surprising changes in physical properties by a long light pre-illumination or by thermo-cycling (with or without external electric field) which produces a memory effects in the ferroelectricity [4] or a strong enhancement and a shift in the intrinsic photoconductivity spectral peak [5]. The results so far known in the TlInS<sub>2</sub> exhibit formation a new shallow donor-acceptor pair (DAP) photoluminescence band after low temperature thermo-cycling [6]. In addition, an imprint of photoactive trap self-polarization in the external electric field under different temperatures was observed and attributed to the dipolar origin of some

\* Corresponding author.

E-mail address: [vytautas.grivickas@ff.vu.lt](mailto:vytautas.grivickas@ff.vu.lt) (V. Grivickas).

unknown intrinsic defects [14]. However, there is a lack of works devoted to the intrinsic PL study in TlInS<sub>2</sub>.

Most previous PL studies were performed on as-grown self-compensated TlInS<sub>2</sub> crystals for the normal k||c incidence to the layer plain by using the standard steady-state experiment setup and a long distance aperture [6,8–13]. One of the most relevant is the work of Karotki et al. [9] performed on thin (~2 μm) samples cleaved from bulk ingot. The band edge transmission, reflectance, PL and the PL excitation spectra were examined at 4.2 K. Authors of Ref. [9] have associated a single narrow PL line with the bound exciton, and few higher ones to direct band gap free exciton split by the polariton coupling. Since the ground state (2.553 eV) had an exact energy with the transmission minimum, the exciton binding (~21 meV) was extracted by a standard procedure of bulk ionic semiconductor using position of the excited exciton state. Though, the optical data obtained by other researchers were containing contradictory PL lines [8,10–13]. Thus, interpretations provided in [9] and in other works assumed coexistence of polymorph inclusions varied in samples which can influence slightly different band gaps.

In the recent study by spectroscopic phase modulated ellipsometry (SPME) the authors extracted direct exciton absorption under the lateral k⊥c incidence for polarization E||c in a wide range of temperatures [2]. The exciton was described by 2D model of dielectric functions. Its energy was 100 meV lower of that observed at the k||c incidence [10] and exciton binding energy was as large as 70 meV in N- and F-phases but reduced to 45 meV near 200 K. The increase of the static in-layer plain dielectric screening at the I-phase was proposed to be responsible for such behavior. Our previous study on the isostructural TlGaSe<sub>2</sub> compound has shown that the intrinsic PL band at RT under the k||c incidence is strongly polarized implying out-of-layer plain oriented e-h dipoles [7].

This work is an attempt to solve some of contradictory results for the TlInS<sub>2</sub> crystals. By means of the confocal microscopy (CM) we extend our previous PL study [7] down to 24 K. The CM microscopy allows measurement on a small micrometer spot size collecting light by a large aperture angle with increased detection sensitivity. CM approach also allows measurement on selected position of the lateral surface with changing excitation light polarization in respect to crystallographic axis. In this work, intrinsic PL spectra were examined in the undoped sample as well as some full-grown with Ag-, B- and Er-atoms.

## 2. Experimental

TlInS<sub>2</sub> single crystals were grown by the modified Bridgman method from a stoichiometric melt. The elemental composition of the crystals was controlled by the energy-dispersive X-ray (EDX) analysis using a LEO 1455 VP and an Apollo 300 scanning electron microscope (SEM). Constituent atoms (Tl, In and S) are in deviation within 1% from the stoichiometric composition. The incorporation of Ag, B, Er was carried out by addition to the melt with molar concentrations of atoms in the range of 0.1–0.5%. As noted previously [7,12,14,15], the incorporation of doping to this level maintain the atomic ratio of constituent elements. The crystals were cut onto parallelepiped pieces normal to the sample plain with a lateral size of a few millimeters and thickness up to hundred micrometers. The resulting lateral surfaces were simply broken from thinner cleaved samples pieces. SEM measurements showed that the doped samples also contain 1–5 μm plain terraced layered microstructure on lateral faces similar as seen of undoped crystals.

The sample was placed on a cold finger of the cryostat and PL spectra were measured with a Nanofinder HE (Lotis TII, Belarus-Japan) CM. The DPSS CW laser (473 nm or 2.62 eV) was used as an excitation source. The incident light was attenuated to avoid a

thermal damage. The PL light was dispersed by a single-grating spectrometer in the backwards direction and registered with a cooled silicon CCD detector with a resolution better than 0.1 nm (0.5 meV). The signal acquisition time was varied from 1 to 30 s. Spectral calibration during measurements was done using a built-in gas-discharge lamp providing an accuracy better than 0.1 nm. An excitation spot area was set to one micrometer. Only visually homogeneous region on surface have been examined.

Three different experimental geometries were used for PL measurement. The wave-vector of the exciting radiation was either parallel (k||c) or normal (k⊥c) to c-axis. In the k⊥c case, the excitation light polarization could be set to be either parallel (E||c) or normal (E⊥c) in respect to the c-axis while in the k||c case the polarization is always normal to the c-axis (E⊥c). In this way, a configuration to exciting light incidences and polarization were obtained by rotating the sample.

The transmission spectra were measured by unpolarized light at RT with a MC122 spectrometer (Proscan Special Instruments) at k||c. In this case, the spectral resolution was about 3 nm and the spot diameter was about 2 mm.

## 3. Results

Transmission of TlInS<sub>2</sub> single crystals at RT shown in Fig. 1 demonstrates a sharp absorption increase for quanta energy above 2.27 eV. This value coincides with a customary indirect band gap  $E_G^i$  at k||c obtained by a simple linear extrapolation of the absorption coefficient in the  $(\alpha h\nu)^{1/2}-h\nu$  coordinates [15]. The position of the direct band gap  $E_G^d=2.47$  eV at RT is by 0.2 eV higher than  $E_G^i$ . Value of  $E_G^d$  was obtained customary by a linear extrapolation in  $(\alpha h\nu)^2-h\nu$  coordinates in a narrow energy range above. (The typical map of the results via this method is exposed in Refs. [10,15,18].) We have found that the presence of B and Ag doping atoms in TlInS<sub>2</sub> give reduction of the transmission below  $E_G^i$ . A small tail is observed down to 1.7 eV for the B doping, and a strong one, down to 1.35 eV, for Ag doping. The last is similar to bands observed for the isostructural semiconductors after Fe doping in TlGaS<sub>2</sub> [16] and in TlGaSe<sub>2</sub> [17]. However, we have found that the Er incorporation does not show an evidence for sub-gap absorption. A flat transmission in all spectral range below  $E_G^i$  can be related to the enhanced light scattering. The Er doping also do not reveal noticeable affect on position of indirect band edge while a small influence perceived with the B and the Ag incorporation.

Fig. 2 demonstrates PL spectra at RT at identical excitation conditions. All measurements where produced on a favorably

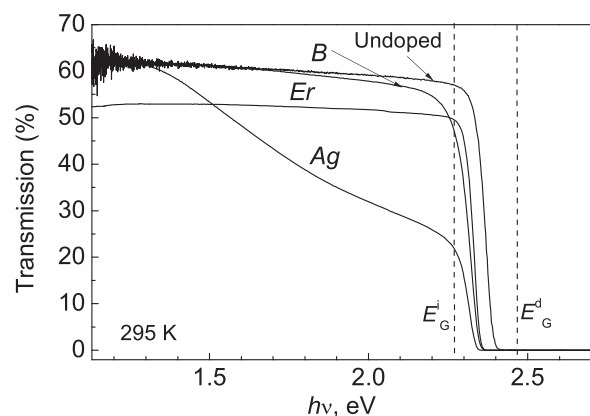
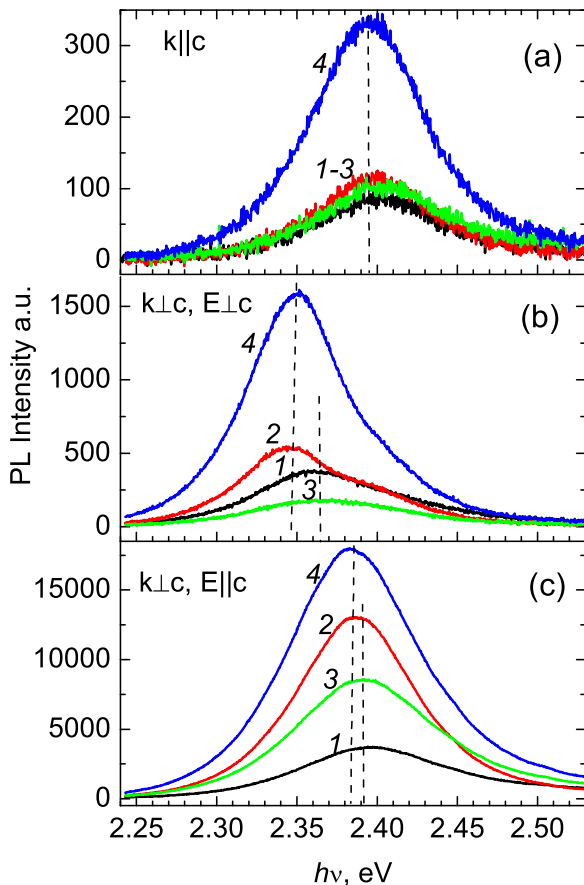
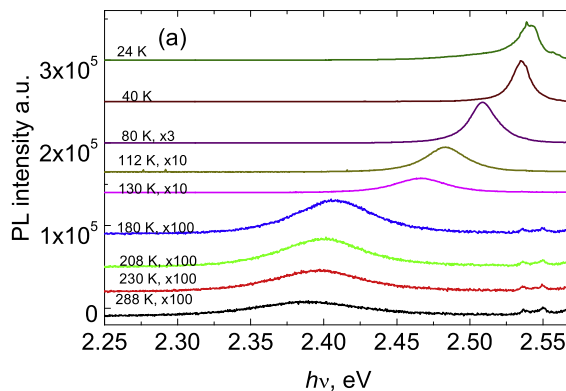


Fig. 1. Transmission spectra for the undoped and the boron, silver and erbium doped TlInS<sub>2</sub> single crystals in the k||c measurement geometry. Vertical dashed lines show customary position of the indirect  $E_G^i$  and the direct  $E_G^d$  band gap of TlInS<sub>2</sub> established at room temperature [10,15,18].

emitting spot in each sample. The emission range is extended in the spectral range between 2.25–2.55 eV. We found, as in the previous report [7], that the PL emission intensity highly depends on the exciting light incidences and light polarization. The labels of ordinate presented in three panels show that the strongest PL emission is detected at the lateral incidence  $k_{\perp c}$  for  $E_{\parallel c}$  polarization (Fig. 2c) which is about a ten time stronger than for  $E_{\perp c}$  polarization (Fig. 2b). Besides, despite the fact that polarization from the lateral light incidence ( $k_{\perp c}$ , Fig. 2b) is the same as from the normal incidence ( $k_{\parallel c}$ , Fig. 2a), the five times strengthen PL



**Fig. 2.** PL spectra of TlInS<sub>2</sub> single crystals measured at RT: 1 – undoped, 2 – Ag doped, 3 – B doped, 4 – Er doped. Excitation: 473 nm/80  $\mu$ W, acquisition time 30 s. The intrinsic PL peak energy position is exaggerated in Fig. 3 by a few vertical dashed lines.



intensity is detected from the lateral side. Moreover, we detected substantial change on PL shape in the last case. That is, at  $k_{\perp c}$ ,  $E_{\perp c}$ , the detected PL shape is asymmetric with a pronounced low energy peak around 2.35 eV and a high energy shoulder part just below 2.4 eV. Whereas in two other configurations (Fig. 3a, c) the spectral shape is close to a single Gaussian settled just a little below of 2.4 eV.

As can be seen in Fig. 2, in the doped and undoped TlInS<sub>2</sub> samples the PL remains of quite a similar shape. The extracted PL Gauss peak energy maxima at RT are outlined in the Table 1. The presence of boron and silver do not diminish PL intensity (panels Fig. 2a,b) but produce PL enhancement at  $k_{\perp c}$ ,  $E_{\parallel c}$  (Fig. 3c), e.g. where virtually the highest PL emission is detected. However, we observe strong enhancement due to the Er incorporation which is clearly detected at all excitation configurations. The PL in Er containing sample is typically stronger by a factor of 3–10 at RT while it increases into the 10–60 fold at low temperatures (not shown). The factor much depends on a particular spot position. For this reason, we did not carry out a detailed study with decreasing temperature.

The Fig. 3a shows PL spectra at the normal  $k_{\parallel c}$  incidence in undoped TlInS<sub>2</sub> measured on a single excited spot with lowering temperature. As expected, a blue shift arises due to the energy gap expansion. At temperatures below 100 K we detected also the DAP emission bands, as typically observed [6,8,9,11,13]. For presented measurement point in Fig. 3a, the DAP can be distinguished hardly since its magnitude is an order lower than the intrinsic PL. In a few places on same sample, however, the DAP increased substantially exhibiting clustering of impurity species. Fig. 3b at 24 K demonstrates the PL maxima intensities versus the excitation laser power in one of such measured position. Both intrinsic and the DAP PL magnitudes increase nearly linearly at low excitation power but saturate and decrease at high power. PL magnitudes are reversible up to 7 mW excitation. The intrinsic PL peak was gradually shifting to the blue side above 1 mW (not shown). At power higher than

**Table 1**

Position of PL peak at 295 K of TlInS<sub>2</sub> single crystals. \* Main maximum according to fitting by two Gaussian curves.

Dopant	Configuration geometry and parameter in eV		
	$k_{\parallel c}$	$k_{\perp c}$ , $E_{\perp c}$	$k_{\perp c}$ , $E_{\parallel c}$
1. Undoped	2.403	2.359*	2.397*
2. Ag	2.399	2.342*	2.387
3. B	2.407	2.368*	2.392*
4. Er	2.395	2.348*	2.384*

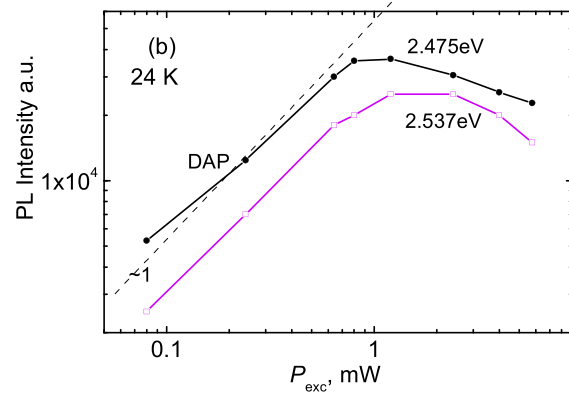


**Fig. 3.** (a) Normalized PL spectra of undoped TlInS<sub>2</sub> crystal in the temperature range 24–288 K measured at  $k_{\parallel c}$ . Excitation: 473 nm/0.8 mW, acquisition time 30 s. The curves are shifted along Y-axis for clarity; (b) The PL intensity versus excitation power at 24 K on a double-log scale. The measurement is produced on a point which exhibits the intrinsic PL peak (2.537 eV) together with DAP (peak at 2.475 eV).

7 mW a time dependent degradation of PL was observed.

Similar kind of high power phenomena was reported in  $\text{TlInS}_2$  previously and perhaps has a common origin. With a similar 476 nm cw-light, by Alkhverdiev et al. [11] – the saturation on the intrinsic PL band was observed at 14 K and, independently, by Aydinli et al. [13] – the saturation occurred on the DAP spectrum at 12 K. On the other hand, a permanent degradation of the intrinsic PL line after continuous cw-light (325 nm at 8 K) was reported in Ref. [9] at 4.2 K. Assuming that PL is excitonic in nature and that  $e$ - $h$  pairs charges are underlying on separate layer we infer that these effects arise because of combination of the build-in electric fields. Electrical fields enhance carrier penetration through PSF potential with increasing nonradiative recombination rate. Non-radiative rate is in competition to a geminate exciton or to a distant donor-acceptor pair and kills radiative emission. The concept can be supported by time-resolved study in the isostructural  $\text{TlGaSe}_2$  where sudden nonradiative lifetime reduction was detected above excited concentration level of  $10^{17} \text{ cm}^{-3}$  at 300 K and 77 K, respectively [19]. Looking for a possible reason on the build-in plain electric field formation we tentatively deduce that  $e$ - $h$  pairs separation are encountered near the inherent PSF defect subsystem. The density of PSF defects is typically high and a subsystem of one PSF per every four layers was testified by McMorro et al. in  $\text{TlGaSe}_2$  [20]. In either case, the high power excitation phenomena will be thoroughly discussed elsewhere.

Let us now turn to a linear PL excitation range and to published exciton absorption data at the  $k||c$  incidence. Fig. 4a presents the PL peak energy with increasing temperature measured at 0.8 mW in the undoped  $\text{TlInS}_2$  (large open circles). At this excitation power we may neglect nonlinear effects. The exciton absorption peak  $E_x^d$  [3,9,10,12] and the estimations of the indirect gap position [18] are shown by various symbols specified in the figure caption. The  $E_x^d$  data of Refs. [3,12] coincide into a common dependence shown by a thin line. Few points of Ref. [9] (stars) and of Ref. [12] (cross) at  $T < 70 \text{ K}$  show some deviation. At the moment the reason of such discrepancy is not clear and we do not take last points into consideration. The comparison in Fig. 4a reveals grounds for a Stokes shift between the emitted PL and the direct exciton absorption peak energy existing in a wide range of temperature. (While PL still is substantially above of  $E_G^i$ .) The observed Stokes shift is 30–35 meV when the crystal is in a weak F-phase below 50 K. Nevertheless, it increases gradually with increasing temperature over the commensurate F-phase and exceeds the maximum of about 80 meV at the transition into the I-phase. (The I-phase region is marked in Fig. 5a by two vertical dashed lines.) In the paraelectric N-phase ( $T > 216 \text{ K}$ ), the shift is roughly at about a

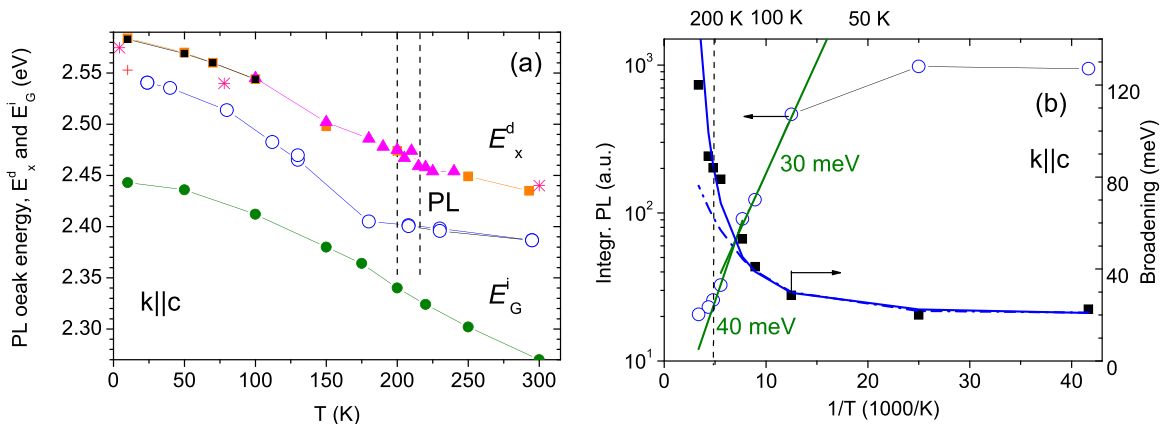


**Fig. 4.** (a) Intrinsic PL energy position versus  $T$  in the undoped  $\text{TlInS}_2$  at  $k||c$ . The CM results – large open circles. The direct exciton absorption  $E_x^d$  is displaced (sol. squares [3], sol. triangles [10], stars [9], a cross [12]). The indirect band gap  $E_G^i$  (solid circles) was estimated in [18]. Vertical dashed lines show the I-phase range 200–216 K. (b) Measured integral PL and its broadening  $\Gamma$  at  $1/e$  versus inverse temperature. Two solid lines with thermal activation of 30 meV and 40 meV are applied in the quenching region of integral PL. The fit to broadening (dashed-dotted line) is made by the Bose-Einstein factor (dashed-dotted line) and by a quadratic equation (solid line), see the text.

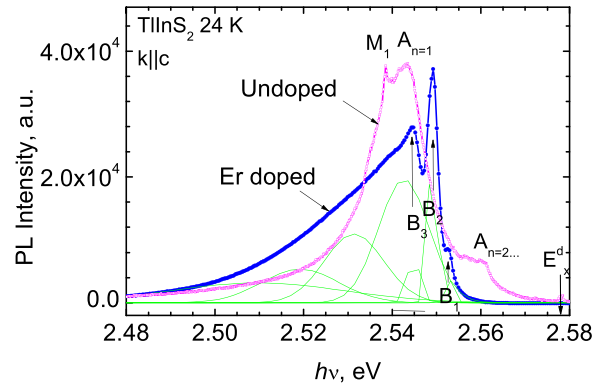


**Fig. 5.** PL spectra of undoped (magenta) and Er doped (blue)  $\text{TlInS}_2$  crystal measured at 24 K in the excitation direction  $k||c$ . Fitting by a set of Gauss lines (green) is given for the Er doping (see also Table 2). Excitation: 473 nm/0.8 mW, acquisition time is 1 s (for Er doped crystal) and 30 s (for undoped crystal).

constant of 40 meV. It is thus tempting to ascribe the presence of this Stokes shift to formation process for 2D-excitons which became ‘indirect’ in real space.

Fig. 4b presents the integral of the PL band intensity and its broadening  $\Gamma$  at  $1/e$  value on the Arrhenius plot. The PL intensity is quenching and broadening expansion starts above 50 K. The quenching can be fitted by thermal activation energy 30 meV in the range 80–150 K which however increases to 40 meV approaching the I-phase transition. Thermal activation is typically attributed to the binding energy of exciton. And the values obtained are substantially higher to that obtained on the excitonic absorption [3,9]. At low temperature the PL band broadening  $\Gamma$  saturates to 23 meV. This value is three times wider than that estimated in the exciton absorption spectrum [3]. The fit to broadening can be obtained by a standard Bose-Einstein factor  $\Gamma = \Gamma_0 [1 + (2 / (\exp(\Theta/T) - 1))] + \Gamma_1 \text{ eV}$  with  $\Gamma_0 = 23 \text{ meV}$ ,  $\Gamma_1 = 0$ , and the average frequency for phonons  $\Theta = 150 \text{ K}$ . It satisfies the broadening dependence up to  $T = 150 \text{ K}$  as shown in Fig. 4b by the dashed-dotted line. More general fitting in all investigated temperatures can be obtained using a quadratic equation of the following type [21]:  $\Gamma = 0.02 + (1.5 \cdot 10^{-6})T^2 \text{ eV}$  (solid line) since it gives a better fit to the data.

PL spectra measured at low temperature (Fig. 5) demonstrate a complex structure containing sharper high-energy components. We identify important difference in PL line structure in the undoped and the Er containing crystal. The undoped crystal spectrum has a rough similarity to that published at 4.2 K in Ref. [9].

**Table 2**  
Position and FWHM of the Gauss lines used for fitting of PL spectrum of Er doped TlInS<sub>2</sub> crystal at 24 K.

No	Peak position, eV	FWHM, meV
B1	2.553	1.7
B2	2.549	2.1
B3	2.545	2.9
B4	2.543	11.4
B5	2.531	13.5
B6	2.519	17.5
B7	2.510	39.2

Following similar notations, we assign the narrowest peak observed M<sub>1</sub> (2.537 eV) to a bound exciton and a double 5 meV split structure labeled A<sub>n=1</sub> above it to the ground exciton states. The structure 16 meV higher above, is labeled by A<sub>n=2</sub>, and can be assigning to excited excitons. The incorporation of Er, nevertheless produces another set of PL spectra. Those can be extracted by set of Gauss lines as indicated by B<sub>i</sub> and shown in Fig. 5 in the green color. The position and FWHM of those components are listed in the Table 2. Three narrow lines B<sub>1</sub> – 2.553 eV, B<sub>2</sub> – 2.549 eV, and B<sub>3</sub> – 2.545 eV have FWHM from 1.7 to 2.9 meV. Those lines can be attributed to a kind of no-phonon emitting excitons. Broader wings B<sub>4</sub>–B<sub>6</sub> have FWHM of 11.4–17.5 meV and can be related to phonon-assisted peaks due to electron-phonon coupling. The strength of the coupling and phonon energies involved thus are different. These facts imply that B<sub>1</sub>–B<sub>3</sub> excitons obey different orientation angle across the layer plain where active phonon at the center of Brillouin zone varies [12]. The line B<sub>7</sub> is much wider (~40 meV) and, as noticed in [9], can be related to a shallow type DAP instead.

The B<sub>4</sub>–B<sub>7</sub> components coincide with tail PL part of the undoped sample. Presence of phonon-assisted components may cause a total red-shifting in PL peak of about 10 meV. This is less of the total 37 meV difference from the published direct exciton absorption energy. This position (see Fig. 4a at 24 K) is indicated in Fig. 5 by down oriented arrow at E<sub>x</sub><sup>d</sup>.

#### 4. Discussion

Before setting the luminescence property, we have to describe how the incident photon at 473 nm, invoked above, can influence the intrinsic PL band in TlInS<sub>2</sub>. We should keep in mind that the crystal structure at 300 K is in the N-phase providing a quasi-uniaxial optical absorption character in respect to *c*-axis [2]. The incident photon energy falls 0.2 eV above E<sub>x</sub><sup>d</sup> into the plateau of the direct band continuum states resulting to constant coefficient of 10<sup>3</sup> cm<sup>-1</sup>. The homogeneous absorption for in-layer-plain polarization was experimentally proved in the isostructural TlGaSe<sub>2</sub> [22]. In the last compound, however, an enhanced absorption rate was detected for illumination through the lateral facet by the depth-resolved measurement [7]. The enhancements subsisted on large spectral area above/below the band gap under the depth exceeding tens of micrometers from the lateral surface [7]. Subsequently, the effect was explained by structure crumpling which has a twofold effect - concentrates the optical field into layers and results in a modification of the states at the extremes of the bands, thereby increasing the absorption rate. It is likely that enhanced optical absorption also exists on the lateral TlInS<sub>2</sub> surfaces. If this anticipation is correct, the excitation increment, similarly to TlGaSe<sub>2</sub>, can be a major reason for the PL increase in Fig. 2b and *c* in respect to the identical excitation condition in Fig. 2a at k||*c*.

The generation rate increment, though, cannot explain the PL peak energy appearance at 2.35 eV in Fig. 2b. Present findings

show that energy reduction subsists in both doped and undoped samples, supporting the concept that the emission property is caused to the crumpled structures of lateral surfaces [7]. The crumpling may lead also to small variations between the bonding angles of corner-connected In<sub>10</sub>S<sub>10</sub> polyhedron units and results from interlayer stress relaxation. Depending on surrounding medium the photon density in close proximity to the exciton emitter is leading to lower emission energy. From Fig. 2b we see, however, that 2.4 eV shoulder subsists on the PL spectral shape (Fig. 2b) which implies that not all structure units are in such disorder and some of them still emit around 2.4 eV. It is significant to point out that 100 meV shift of the exciton absorption at k||*c* (acting in all temperatures from 100 K to 400 K) was presented by Mamedov et al. [2]. These results were obtained on the smoothly polished lateral surface of the TlInS<sub>2</sub> [2] at E||*c* and double exceeds our present finding.

The result that doping impurity incorporation in TlInS<sub>2</sub> matrix generally intensifies the intrinsic PL emission (Fig. 2) can be explained as follows. We assume that B and Ag (like Fe in TlGaSe<sub>2</sub>) provide partial substitution of the host atom (or a kind of interstitial) creating energy levels in the forbidden band gap. At the same time, like Fe in the TlGaSe<sub>2</sub> for the molar ratio less of 0.5% these impurities basically do not affect the direct band absorption [17]. Simple calculation shows that a large part of incorporated impurity atoms in the growing mixture of the melt segregate in various places of the layered crystal in a form of small clusters or precipitates. Incorporated particles change the interlayer stresses which occurs due to numerous PSF defects of layered structure. It is well known that rare-earth elements like Er are characterized by a low solubility. Fig. 1 implies that Er inclined only to form particles creating light scattering but not absorption below indirect band gap. Thus we expect that Er more than B or Ag can provide relaxing of overall interlayer stresses and can support the preference for the 2D-exciton formation. The effect is particularly active in the case E||*c* (Fig. 2c) where layered structure supports intrinsic property with higher radiative decay rate. We should note that intrinsic PL intensity increase was also observed by us for the isostructural TlGaSe<sub>2</sub> in the case of incorporation of rare-earth element Terbium.

In the F-phase, the layered crystal loses the quasi-uniaxial character due to Tl<sup>+</sup> ions sliding out of *a,b* crystallographic lines. Currently, this Tl<sup>+</sup> slippage is most common explanation for occurrence of the F-phase in layered Tl-based semiconductors [1]. The validation of this phenomenon was proven theoretically as long as 1959 by Orgel [23] showing energetically favorable Tl:6p and Tl:6s orbital mixing of nearby Tl ions. Hochheimer et al. [24] and Yee and Albright [25] were the first to draw attention to this problem investigating the bonding and coordination number of corner Se atom structure in TlGaSe<sub>2</sub> at low temperatures. Therefore the x-ray analysis has shown that structure basically is keeping the same temperature dependence of the unit cell volume [24]. The absorption anisotropy of the direct band gap in TlGaSe<sub>2</sub> at 77 K was experimentally measured in Ref. [22]. While no data exist in TlInS<sub>2</sub> so far, we expect that crystal has few absorption maxima across the layer depending on Tl-ion configurations since Tl atom (as well as In) in the F-phase has structurally inequivalent positions on a single unit cell [26]. We expect that excitons labeled A in Fig. 5 for undoped TlInS<sub>2</sub> sample can be dipole orientated out-of-plain in two directions with slightly different Bohr radius. This explanation should be more natural in respect of idea of the polariton coupling (proposed in [9]) because last one process needs quite a strong light-exciton interaction [27]. The fact that different exciton states are detected in Er-doped TlInS<sub>2</sub> implies that its position is strictly dependent on the interlayer stresses. More investigation should be performed to prove issue of this statement both experimentally and theoretically.

In view of the discovered fact that at configuration kllc (Fig. 4a) where persist the pronounced Stokes shift between PL peak and the exciton absorption  $E_x^d$  and that exciton parameters extracted differ substantially implies that two mechanisms have a quite different origin. We should note that TlInS<sub>2</sub> crystal between T=4–300 K is in different structural phases. One can identify the temperature coefficients and show that the transition energy and the line broadening are irregular functions of temperature in each phase, respectively. In either case the one exciton state is acting during the photoexcitation process and the latter exciton during photon emission. Both processes are delayed in time. The transformation may occur if *e-h* pair separation is not instant and persists on a time scale. Then, after transformation, the exciton jumps into lower energy state, which is characteristic of the 'indirect' real space. The later process can be considered as a self-trapping process under the existing internal stress in the layered structure. This transformation process of the exciton formation definitely calls for more detail studies on the femto-to-picosecond time scales.

## 5. Summary

We have studied intrinsic PL transition in layered TlInS<sub>2</sub> by CM spectroscopy in a wide range of temperatures. The obtained data at kllc show that the Stokes shift of 30–80 meV between the PL peak energy and the published direct exciton absorption energy exists at different crystal phases. The low temperature measurements show that presence of phonon-assisted components can explain only one quarter of the Stokes shift. Thus we propose that the shift can be understood in terms of 2D-exciton rearrangement across layers occurring on a delayed time scale. The enhancement of PL intensity at RT from the lateral surface is caused mainly by the incident light absorption enhancement. At klc, E<sub>lc</sub> the position of the RT PL band is intended to be determined by the structure crumpling near lateral surface. The incorporated impurities, particularly Er, enhance the emission intensity in the intrinsic PL band. This phenomenon is interpreted by impurity acting on the interlayer stress reduction in layered structure. At 24 K, disparity in fine structures of PL spectra for undoped and Er doped TlInS<sub>2</sub> single crystals can be interpreted by appearance of stress relaxed configuration. The saturation/reduction of intrinsic PL and DAP with increasing laser power is explained using steep increase of the nonradiative recombination rate. Presented ideas do not involve in the explanation coexistence of polymorph inclusions in layered TlInS<sub>2</sub> samples. Therefore, the internal stresses are assumed to be caused by PSF defect subsystem. The potential value and shape of the barrier is the main open question for future studies in order to understand properties of layered TI-based semiconductors.

However, an exfoliation to single layers in TlInS<sub>2</sub> is more difficult in respect to the MoS<sub>2</sub>, MoSe<sub>2</sub> dichalcogenides [28].

## Acknowledgement

This work was funded by a common Grant (S-LB-2017-1) from the Research Council of Lithuania and the State Committee of Science and Technology of Belarus Republic.

## References

- [1] A.M. Panich, *J. Phys.: Condens. Matter* 20 (2008) 3.
- [2] N. Mamedov, Y. Shim, W. Okada, R. Tashino, K. Wakita, *Phys. Stat. Sol. B* 252 (2015) 1248.
- [3] J.A. Kalomirois, A.N. Anagnostopoulos, *Phys. Rev. B* 50 (1994) 7488.
- [4] M. Yu. Seydov, F.A. Mikailadze, T. Uzun, A.P. Odrinsky, E. Yakar, V.B. Aliyeva, S. Babayev, T.G. Mammadov, *Phys. B* 483 (2016) 82.
- [5] S. Ozdemir, M. Bucurgat, *Sol. Struct. Sci.* 33 (2014) 25.
- [6] H. Uchiki, D. Kanazawa, N. Mamedov, S. Iida, *J. Lumin.* 87–89 (2000) 664.
- [7] V. Grivickas, K. Gulbinas, V. Gavryushin, V. Bikbajevs, O.V. Korolik, A. V. Mazanik, A.K. Fedotov, *Phys. Stat. Sol. – Rapid Res. Lett.* 8 (2014) 639.
- [8] T. Arai, J. Aoyagi, Y. Maruyama, S. Onari, K.R. Allakhverdiev, E. Bairamova, *Jpn. J. Appl. Phys.* 32 (Suppl. 32-3) (1993) S754.
- [9] A.V. Karotki, A.U. Sheleg, V.V. Shevtsova, A.V. Mudryi, S.N. Mustafaeva, E. M. Kerimova, *J. Appl. Spectrosc.* 79 (2012) 398.
- [10] Y. Shim, Y. Nishimoto, W. Okada, K.K. Wakita, N. Mamedov, *Phys. Stat. Sol. C* 5 (2008) 1121.
- [11] K.R. Allakhverdiev, N.M. Gasanly, A. Aydinli, *Sol. (St.) Struct. Commun.* 94 (1995) 777.
- [12] V.V. Zalamai, I.G. Stamo, N.N. Syrbu, V.V. Ursaki, V. Dorogan, *J. Luminesc.*, 160, 20150, 195.
- [13] A. Aydinli, N.M. Gasanly, I. Yimaz, A. Serpenguzel, *Semicond. Sci. Technol.* 14 (1999) 599.
- [14] M. Yu. Seydov, R.A. Suleymanov, F.A. Mikaladze, E.O. Kargin, A.P. Odrinsky, *J. Appl. Phys.* 117 (2015) 224104.
- [15] N.M. Gasanly, *J. Appl. Phys.* 118 (2015) 035701.
- [16] B. Gürbulak, *Phys. Stat. Sol. A* 184 (2001) 349.
- [17] V. Grivickas, V. Gavryushin, P. Grivickas, A. Galeckas, V. Bikbajevs, K. Gulbinas, *Phys. Stat. Sol. A* 208 (2011) 2186.
- [18] N.M. Gasanly, *J. Korean Phys. Soc.* 57 (2010) 164.
- [19] V. Grivickas, A. Odrinski, V. Bikbajevs, K. Gulbinas, *Phys. Stat. Sol. B* 250 (2013) 160.
- [20] D.F. McMorrow, R.A. Cowley, P.D. Hatton, J. Banys, *J. Phys.: Condens. Matter* 2 (1990) 3699.
- [21] P. Lautenschlager, M. Garriga, L. Vina, M. Cardona, *Phys. Rev. B* 36 (1987) 4821.
- [22] K. Gulbinas, V. Grivickas, V. Gavryushin, *Appl. Phys. Lett.* 105 (2014) 242107.
- [23] L.E. Orgel, *J. Chem. Soc.* (1959) 3815–3819.
- [24] H.D. Hochheimer, E. Gmelin, W. Bauhofer, Ch von Schnering-Schwarz, H. G. von Schnering, J. Ihringer, W. Appel, *Z. Phys. B – Condens. Matter* 73 (1988) 257.
- [25] K.A. Yee, Th.A. Albright, *J. Am. Chem. Soc.* 113 (1991) 6474.
- [26] A.M. Panich, S.J. Kashida, *Phys.: Condens. Matter* 20 (2008) 395211.
- [27] I. Pelant, J. Valenta, *Luminescence Spectroscopy of Semiconductors*, Oxford Univ. Press, Oxford, NY, 2012.
- [28] H. Li, X. Wu, H. Liu†, B. Zheng, Q. Zhang, X. Zhu, Z. Wei, X. Zhuang, H. Zhou, W. Tang, X. Duan, A. Pan, *ACS Nano* (2016), <http://dx.doi.org/10.1021/acsnano.6b07580>.